RGNZ/MGPB

Rudarsko-geološko-naftni zbornik
(The Mining-Geology-Petroleum Engineering Bulletin)
DOI: 10.17794/rgn.2025.4.10

Original scientific paper

Assessment of the Severe Geomagnetic Storm on May 10-11, 2024 Effects on the Geomagnetic Field and Ionosphere Over the Indonesian Region

Anwar Santoso[1,2]*, Sismanto Sismanto[3], Rhorom Priyatikanto[1], Eddy Hartantyo[3], Emanuel Sungging Mumpuni[1], La Ode Muhammad Musafar Kilowasid[1], Abdul Rachman[4], Fitri Nuraeni[1], Siska Filawati[1], Erlansyah[1], Dadang Nurmali[1]

[1] *Research Center for Space, National Research and Innovation Agency (BRIN), Bandung 40173, Indonesia.*
[2] *Physics Department, Faculty of Mathematics and Natural Sciences, Gadjah Mada University, Yogyakarta, Center of Java 55281, Indonesia.*
[3] *Geophysics Laboratory, Physics Department, Faculty of Mathematics and Natural Sciences, Gadjah Mada University, Yogyakarta, Center of Java 55281, Indonesia.*
[4] *National Research and Innovation Agency (BRIN), Kupang, East Nusa Tenggara 85362, Indonesia.*

Abstract
The severe geomagnetic storm on May 11, 2024, is the largest space weather phenomenon in the 25th solar cycle. This paper presents the impact of that severe geomagnetic storm (*Dst* = -412 nT) on the geomagnetic field and ionosphere over Indonesia. Additionally, it examines geoelectric disturbances generated during the storm and disruptions to HF radio communication in Indonesia. The study uses geomagnetic field data (HDZ) and ionospheric data (*fo*F2) from Pontianak and Kupang, averaged minutely and hourly. The results indicate that the geomagnetic storm on May 11th, 2024 caused geomagnetic disturbances with ΔH = -471 nT in Pontianak and ΔH = -462 nT in Kupang. These disturbances led to significant geoelectric disturbances around the region with possible induced currents. In the ionosphere, the geomagnetic storm caused negative ionospheric storms during the main phase and positive storms during the recovery phase, as observed in the *fo*F2 data from both stations. These ionospheric storms resulted in *fo*F2 disturbances (ϕ) with values ranging from -30% to 30%, lasting for 180 minutes.

Keywords:
geomagnetic storm, interplanetary magnetic field, space weather, geomagnetic induced current, ionosphere

1. Introduction

The Earth was bathed in a spectacular display of auroras in May 2024, a consequence of a powerful geomagnetic storm that reached a G5 classification - the highest on the geomagnetic storm scale defined by the National Oceanic and Atmospheric Administration (**Kwak et al., 2024**). This event, driven by a series of coronal mass ejections (CMEs) originating from an exceptionally active region on the Sun identified as AR13664 (**Jaswal et al., 2024**; **Kontogiannis, 2024**), marked the most intense geomagnetic storm since the famed Halloween Storms of 2003 (**Gopalswamy et al., 2005**). The storm peaked between May 10th and 11th, with the interplanetary magnetic field (IMF) indicating a sharp increase to 88 nT and a southward component of -50 nT (**Hajra et al., 2024**). Coupled with high solar wind density and speeds reaching 750–1450 km/s, this interplanetary state created ideal conditions for a major geomagnetic disturbance (**Liu et al., 2024**). This resulted in a disturbance storm time *(Dst)* index of -412 nT, indicating a major geomagnetic disturbance. Since its occurrence coincided with International Mother's Day, the storm has been dubbed the "Mother's Day Storm", also known as "Gannon storm" (**Grandin et al., 2024**).

The impact was widespread. Auroras, typically confined to high-latitude regions, were visible as far south as Florida, the Yucatán Peninsula in Mexico, and even the Canary Islands, approximately 30 degrees from the geomagnetic equator (**Grandin et al., 2024**). This stunning visual spectacle, however, was accompanied by disruptions to radio communications and the Global Navigation Satellite Systems (GNSS). While no major power grid failures were reported, the storm served as a potent reminder of the potential for extreme geomagnetic storms to disrupt our technology-dependent world (**Hapgood, 2011**; **Riley et al., 2018**; **Ishii et al., 2024**). While the most dramatic effects of geomagnetic storms are often observed at high latitudes, low-latitude regions are not immune to their influence. The May 2024 storm provided compelling evidence of this influence, with au-

* Corresponding author: Sismanto Sismanto
e-mail address: sismanto@ugm.ac.id
Received: 2 December 2024. Accepted: 14 March 2025.
Available online: 27 August 2025

roras visible in regions far closer to the equator than usual. This highlights the fact that even at low latitudes, geomagnetic storms can cause significant disruptions. Satellites experienced enhanced atmospheric drag that shortened their lifetime (**Parker and Linares, 2024**) while their operations could be disrupted, affecting communication, navigation, and Earth observation systems worldwide. Increased radiation levels during strong geomagnetic storms pose risks to astronauts and passengers on high-altitude flights.

In the ionosphere, geomagnetic storms can cause changes in plasma density, leading to either an increase or a decrease depending on the inherent characteristics. These variations are referred to as positive or negative ionospheric storms (**Horvath and Lovell, 2015**; **Matamba et al., 2015**), both of which can disrupt high-frequency (HF) radio communication. HF is a communication band for civil and military radio services with a frequency range of 3–30 MHz (**ITU, 2015**), which can usually extend to 2–30 MHz (**ITU, 2019**). The operating HF radio systems are usually guided by some parameters such as the Maximum Usable Frequency (MUF), Optimum Working Frequency (OWF) or Frequency Optimum Travail (FOT), Height Probable Frequency (HPF), and Lowest Usable Frequency (LUF) (**ITU, 2007; 2019**). MUF is the product of the critical frequency at the F2 ionospheric layer (*fo*F2) and propagation factor (M(3000)F2). MUF is approximately three times that of critical frequency (**Carr, 2011**). OWF or FOT is approximately 85% MUF (**Goodman, 1992**). MUF HF radio has widespread applications in various fields, such as search and rescue operations, emergency communication, government broadcast, military communication, and radar detection. The largest impact during a storm occurs on traditional means of communication i.e. HF radio (**Wang et al., 2022**).

Specific to the Mother's Day storm, **Karan et al. (2024)** reported a poleward shift of the Equatorial Ionization Anomaly (EIA), which normally persists around 10-20 degrees north and south of the geomagnetic equator (**Balan et al., 2018**). Due to the injection of energy from the solar wind and magnetosphere, this feature changed in shape and moved up to 35° magnetic latitude. There was also evidence that EIA did merge with aurora near the tip of South America. Meanwhile, **Foster et al. (2024)** highlighted a significant increase in Total Electron Content (TEC) over the continental United States along with the auroral extension in this region. Some detectors measured a strong increase of vertical TEC up to 50 TEC units. Another form of ionospheric anomaly was also reported by **Spogli et al. (2024)** for the European region. A negative storm indicated by a decrease in ionospheric density was observed on May 11th and after the recovery phase on May13th. A 30-TEC unit drop of the vertical TEC over the Italian Peninsula was observed on both dates. In addition to that, **Spogli et al. (2024)** also reported a drop of *fo*F2, to a very low value of 2 MHz. At high-latitude regions, the disappearance of the F2 layer was observed during the storm, accompanied by a clear scintillation affecting the GNSS signal transmissions (**Themens et al., 2024**).

Intense storms can induce powerful electrical currents in the Earth's crust, known as geomagnetically induced currents (GICs), which can damage power grids, pipelines, and other critical infrastructure (**Pulkkinen et al., 2017**; **Abda et al., 2020**). The auroral electrojet (AE) is believed to play a critical role in generating GICs at high latitudes (**Ngwira et al., 2013**; **Ngwira and Pulkkinen, 2018**) whereas the equatorial electrojet (EEJ) is suspected to have a significant role in generating GICs at low-latitude regions during geomagnetic storms (**Nilam and Ram, 2022**). Recently, GIC measurements have been carried out in many countries at low and middle latitudes, such as Brazil (**Trivedi et al., 2007**), Spain (**Torta et al., 2012**), Australia (**Marshall et al., 2013**), China (**Liu et al., 2009**), and Japan (**Watari et al., 2009**, **2021**). Depending on the location and the storm intensity, the generated GICs are typically around 10 A or lower. Interestingly, **Zawawi et al. (2020)** conducted simulations using geomagnetic field data from the Langkawi geomagnetic observatory at -2.8 dipole latitude and reported the potential presence of GICs in Malaysia. They estimated that a GIC of 7 A may appear in a 275 kV transmission transformer in Peninsular Malaysia and cause half-cycle saturation, leading to performance issues in the transformer.

Maritime regions like Indonesia face unique challenges during geomagnetic storms. Disruptions to the GNSS and radio communication can affect navigation and safety at sea. Additionally, there is evidence that coupling between the ocean and ionosphere during geomagnetic storms is possible (**Akala et al., 2020**). The increasing reliance on autonomous navigation systems in the maritime industry further emphasizes the need for robust mitigation strategies against the effects of geomagnetic storms.

In this paper, we analyze the geomagnetic field and ionospheric responses over the Indonesian region during the Mother's Day storm. Specifically, we investigate the potential of induced electric fields and disruptions to high-frequency radio communication in this maritime country.

2. Data and methods

Indonesia's location within the low-latitude region makes it a prime location for geophysical and space weather research. The ionosphere above Indonesia, influenced by the equatorial electrojet and unique atmospheric dynamics, plays a crucial role in radio wave propagation (**Abadi et al., 2021**). To support research on the ionosphere and magnetosphere over Indonesia, there are several observing stations located across this archipelago (see **Figure 1**). Previously operated by the National

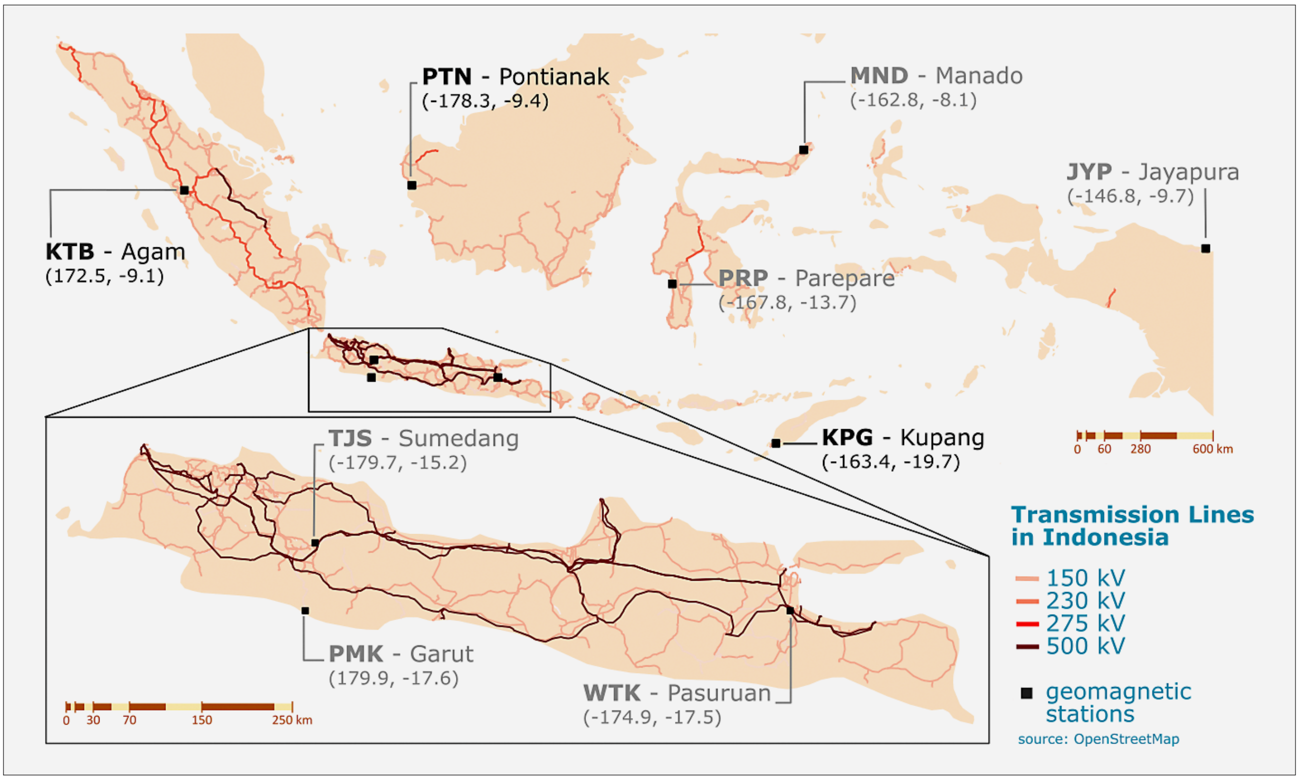

Figure 1. The map (north up) displays the locations of observing stations (squares) in Indonesia, overlaid on a network of electric transmission lines with a capacity of 150 kV or higher. Geomagnetic coordinates for each station are shown in brackets.

Institute of Aeronautics and Space (LAPAN) and now by the National Research and Innovation Agency (BRIN), the stations are equipped with some critical instruments, like a radiosonde and magnetometer.

During the Mother's Day Storm, geomagnetic and ionospheric data for further analyses were acquired from two stations, namely BRIN Pontianak (PTN, 9º S and 177º9' W magnetic or 0º2' S and 109º3' E geographic) and BRIN Kupang (KPG, 19º S and 162º9' W magnetic or 10º2' S and 123º7' E geographic). Data available on request. At these stations, a three-dimensional magnetic field (H, D, Z) was measured using fluxgate magnetometers operated at 1 second, and for the study, we averaged the data into a 1-minute sample. Actually, Agam station in Sumatera Island was operational during the storm, but the data from this station was not used in this study due to quality and validity issues. Data recorded from May 10-15 was analyzed, while the data acquired within a month before the storm was used to establish a base level in the quiet days. Meanwhile, the ionospheric monitoring was conducted using CADI ionosonde so that several important parameters, like *fo*F2, could be derived. The temporal resolution of the *fo*F2 data was 15 minutes.

Preprocessing of the data was done to accentuate the disturbance during the storm. At a particular time, the local disturbance was defined as the observed magnetic field subtracted by the average field strength during 5 quiet days in May 2024. The list of quiet days was obtained from the GFZ Data Services (**Matzka et al., 2021**). More definitely, the following equation was used to determine the disturbance:

$$\Delta H(t) = H(t) - H_{sq}(t) \quad (1)$$

where:

ΔH(t) = the local disturbance geomagnetic field,
H(t) = the observed geomagnetic field at time t,
HSq(t) = the associated value during quiet days.

Meanwhile, preprocessing was also performed on the data produced by ionosonde at PTN and KPG. The ionogram was manually scaled to obtain the *fo*F2. The median value of *fo*F2 in May 2024 ($foF2_{median}$) was considered as the baseline so that the deviation from this baseline could be regarded as a disturbance due to the storm. Considering the daily variation of the *fo*F2, the deviation could also be normalized by the median value to determine the relative disturbance:

$$\phi = \frac{foF2_{observed} - foF2_{median}}{foF2_{median}} 100\% \quad (2)$$

where:

ϕ = disturbed values,
$foF2_{median}$ = the median value of *fo*F2 in May 2024,
$foF2_{observed}$ = the observed value *fo*F2 in May 2024.

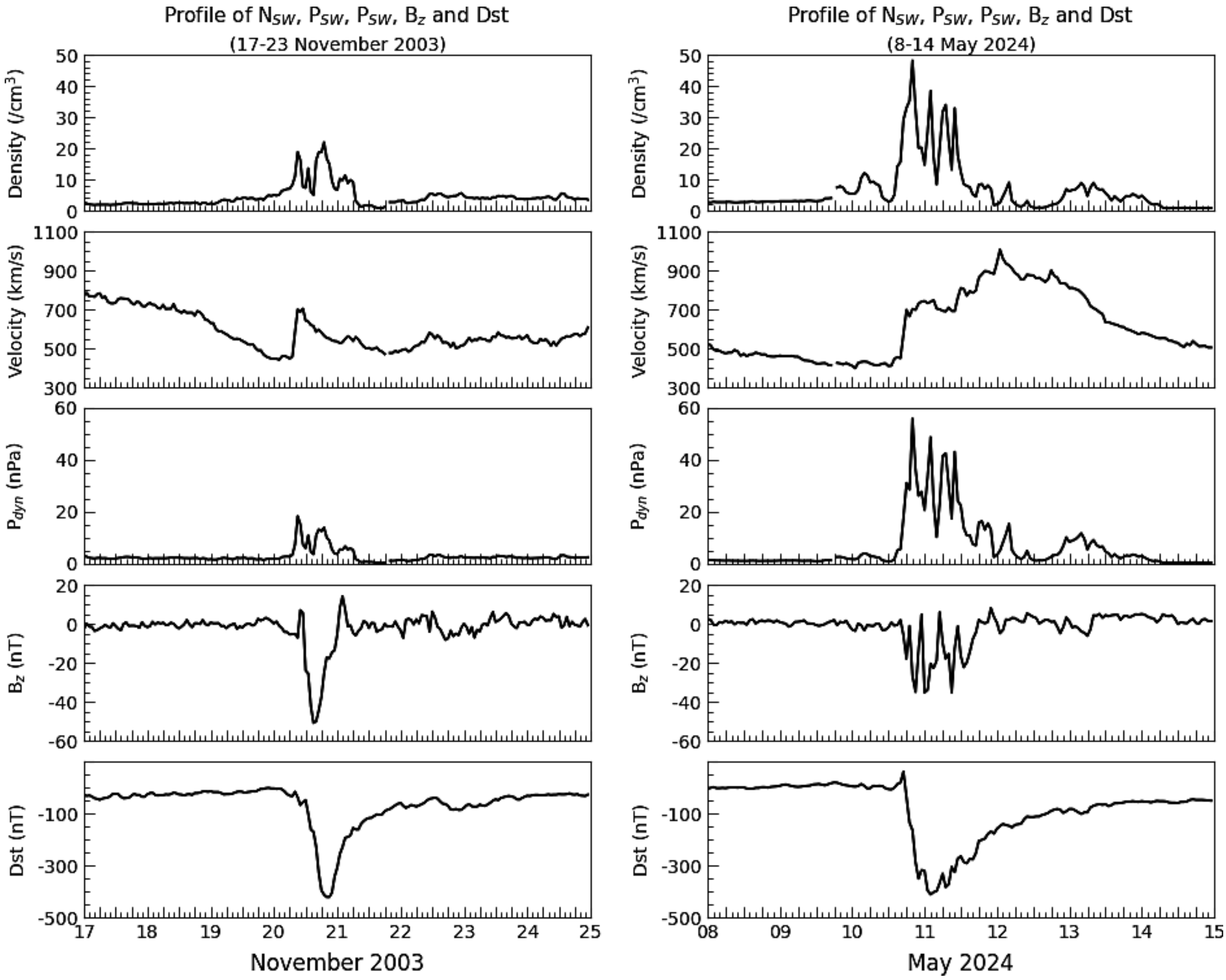

Figure 2. Graphical profile of solar wind parameters, IMF Bz component, and Dst during the geomagnetic storms on November 20, 2003 (left) and May 11, 2024 (right).

3. Geoelectric disturbance

To obtain a first-order estimate of the potential of GIC in Indonesia during the Mother's Day storm, we first estimated the electric field disturbance generated by the varying source fields from the ionosphere. Assuming the source field as a downward propagating plane wave and uniform conductivity at Earth's surface, the following relation is valid (e.g. **Viljanen, 1998**):

$$E_x(t) = \frac{1}{\sqrt{\pi\mu_0\sigma}} \int_{-\infty}^{t} \frac{g_y(u)}{\sqrt{t-u}} du \quad (3)$$

$$E_y(t) = -\frac{1}{\sqrt{\pi\mu_0\sigma}} \int_{-\infty}^{t} \frac{g_x(u)}{\sqrt{t-u}} du \quad (4)$$

where:

μ_0 = denotes vacuum permeability = 4π x 10^{-7} in unit (Wbr/ A. m or Wb A^{-1} m^{-1} or H/m),

σ = represents the Earth's conductivity in unit S/m,

ρ = represents the Earth's resistivity in unit W m and

$g_x(u)$ = dH/dt is the time derivative of the magnetic field along the north-south direction (V/km). The same relation applies for $g_y(u)$ = dD/dt (V/km).

Regarded as the simplest way to calculate geoelectric field due to geomagnetic changes, the plane wave method has some limitations. It does not take into account spatial variation of the ground conductivity. However, this simple method was considerably sufficient to assess the impact of geomagnetic storm in this study. The integration in **Equation 4** was in practice started 10 minutes before the time t and continues every 10 minutes. So **Equations 3** and **4** can be used to estimate the generative potential of an induced electric field.

4. Results

Intense geomagnetic storms, such as the one in May 2024, are rare events. Statistical analysis suggests that G5-level storms (Dst < -250 nT) occur approximately four times per solar cycle (**Tsubouchi and Omura, 2007**). Meanwhile, extreme geomagnetic events with

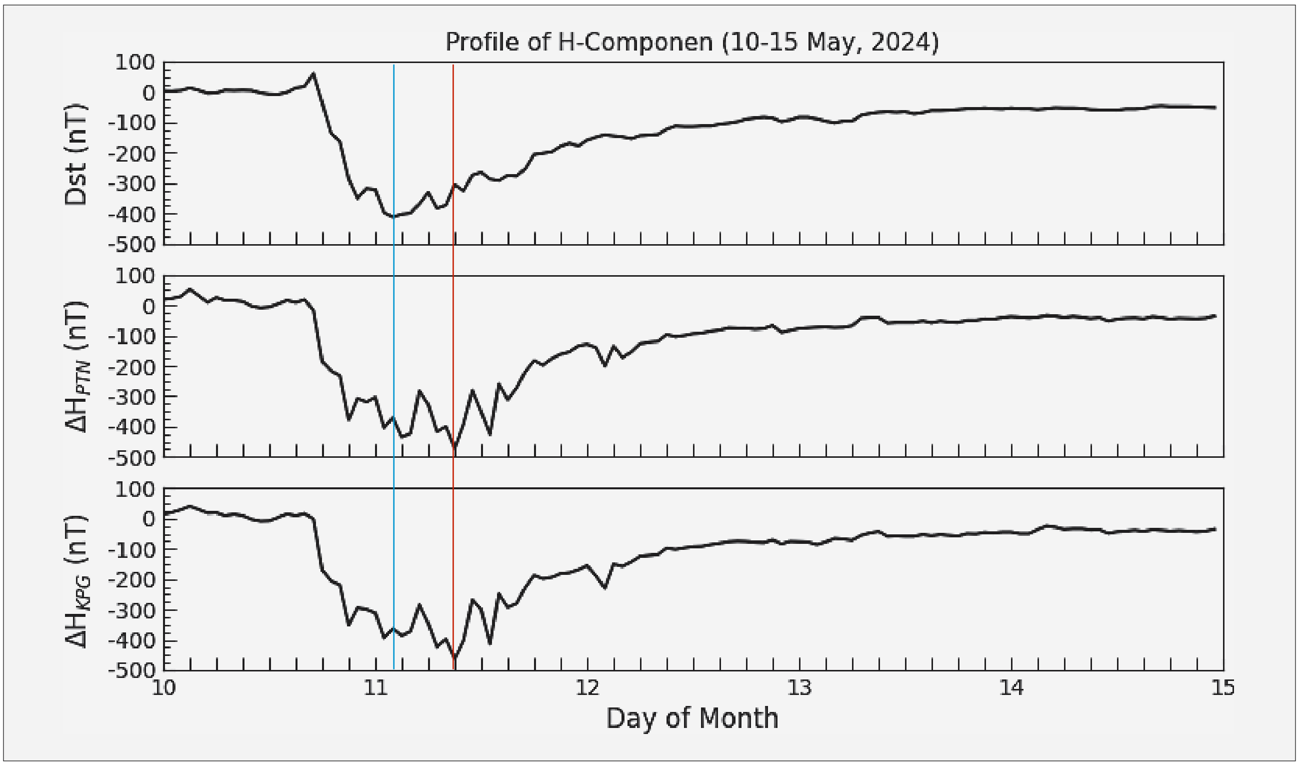

Figure 3. Graphical profile of Dst index (top), the *ΔH* component of the geomagnetic field from Pontianak areas (middle) and Kupang (bottom). The vertical blue line indicates the minimum *Dst,* while the vertical red line indicates the *ΔH* component from both Pontianak and Kupang reaching a minimum.

Dst values around -600 nT possibly occur once per century (**Love et al., 2020**; **Cliver et al., 2022**). However, their unpredictable nature and potential for widespread disruption underscore the importance of continuous space weather monitoring and preparedness (**Schrijver et al., 2015**). The last major geomagnetic storm was on November 20, 2003 (*Dst* = -422 nT). To support space weather monitoring efforts, this study compares the characteristics of the geomagnetic storms on November 20, 2003, and May 11, 2024.

Identification of the Sources of Geomagnetic Storms on November 20, 2003, and May 11, 2024

The geomagnetic storm event on November 20, 2003 (*Dst* = -422 nT at 21:00 UT) was driven by a halo CME associated to M-class flare from active region AR0501 at N00E18 on November 18, 2003, at 07:52 UT, with a travel time to Earth of 47.5 hours. Meanwhile, the geomagnetic storm on May 11, 2024 (*Dst* = -412 nT at 02:00 UT) was generated by halo CME linked to an X2.2-class flare from active region 3664, at S20W26 on May 9, 2024, at 08:45 UT, with a travel time to Earth of 32 hours. The profile of solar wind parameters and *Bz* before the storm (*Dst* index) are shown in **Figure 2**.

Geomagnetic Field and Geoelectric Disturbance in Indonesia

Figure 3 summarizes the severity of geomagnetic disturbances in Indonesia. In Pontianak and Kupang, *ΔH* values dropped to approximately -400 nT, exhibiting fluctuations similar to those observed in the *Dst* index. However, the local data showed fluctuations with greater amplitude. Notably, the minimum DH values occurred approximately six hours after the minimum *Dst* value was recorded.

To assess geoelectric disturbances in Indonesia due to the geomagnetic storm on May 11, 2024 (Mother's Day), we can refer to the Ex and Ey values in **Equations 3** and **4** using input data of the geomagnetic field components *H* and *D* from Pontianak and Kupang. **Figure 4** shows the patterns *of dH/dt, dD/dt, Ex*, and *Ey* at Pontianak and Kupang. There were two episodes of geoelectric enhancements observed: one coincided with the peak of storm and another one occurred during the recovery stage (around May 12 02.00 UT). At both stations, *dH/dt* and *dD/dt* fluctuated with an amplitude of about 3 nT/s, implying geoelectric disturbances of around 10 mV/km. Smaller fluctuations were observed in the second episode. The amplitude was approximately 50% of the one in the first episode while the overall duration was only 3 hours.

Identification of Ionospheric Response and Potential HF Radio Communication Disruptions in Indonesia

To observe the impact of the Mother's Day Storm on ionospheric irregularities in Indonesia, we plotted *fo*F2 data along with the median *fo*F2 for May 2024 and cal-

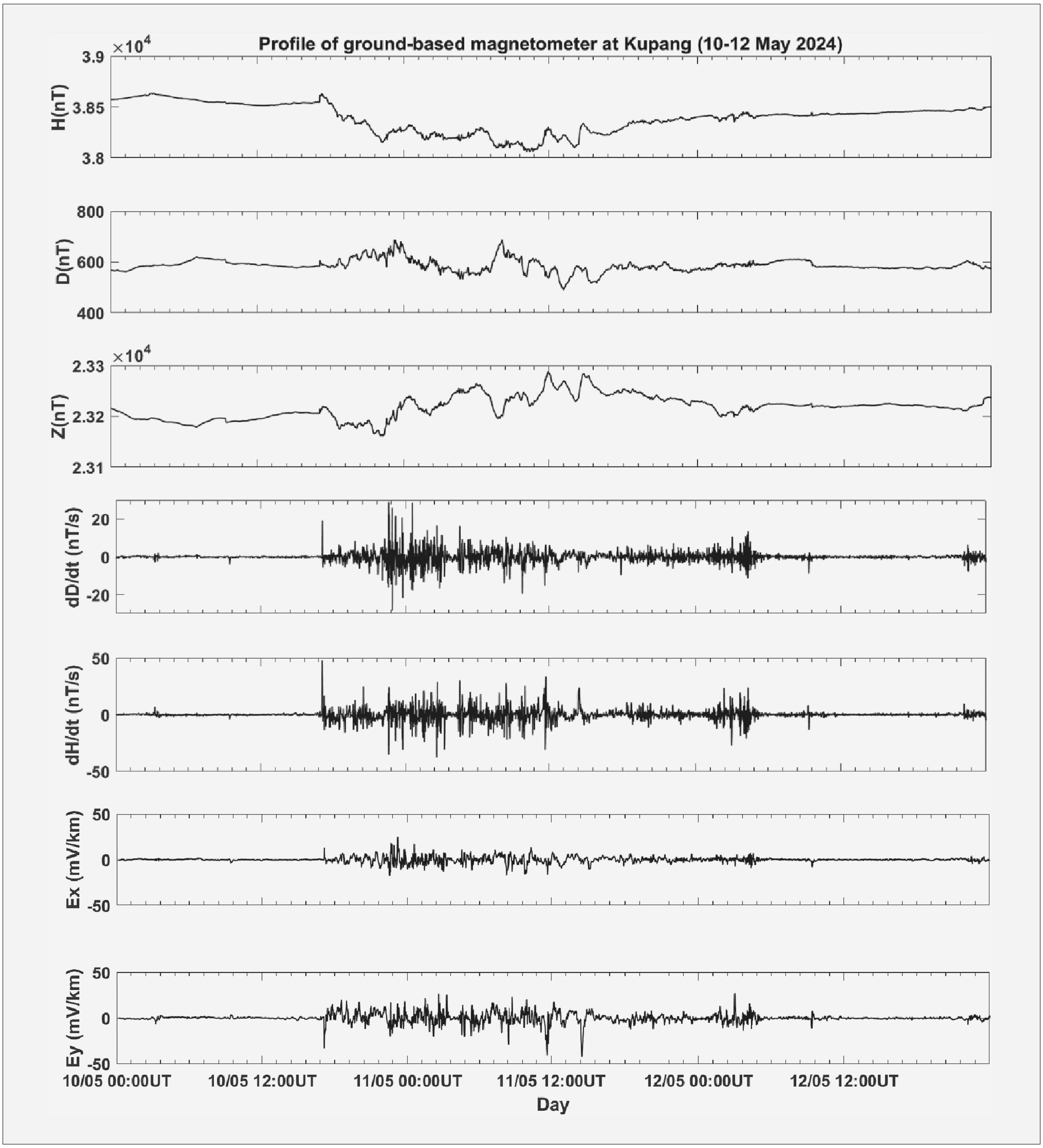

Figure 4. Profile of *dH/dt, dD/dt, Ex,* and *Ey* at Kupang on May 10-12, 2024

culated the ionospheric disturbance value (ϕ) using **Equation 2**. The results of the *fo*F2 data plot and the median *fo*F2 for May 2024 are shown in **Figure 5**.

The variation from the median value with ±30% of the median is shown in **Figure 6**.

4. Discussion

From **Figure 2**, several characteristics of the geospace environment's effectiveness before the geomagnetic storms on November 20, 2003, and May 11, 2024, are summarized in **Table 1**. Based on this data, the geospace environment's effectiveness before the May 11, 2024 storm was more prominent compared to the November 20, 2003 storm. However, due to the stronger *Bz* and ΔT (time lag) values in the November 20, 2003 storm, the *Dst* value was more intense than in the May 11, 2024 storm. Therefore, it is believed that the behaviour of the solar wind parameters, *Bz*, and ΔT, were crucial factors in these geomagnetic storm events.

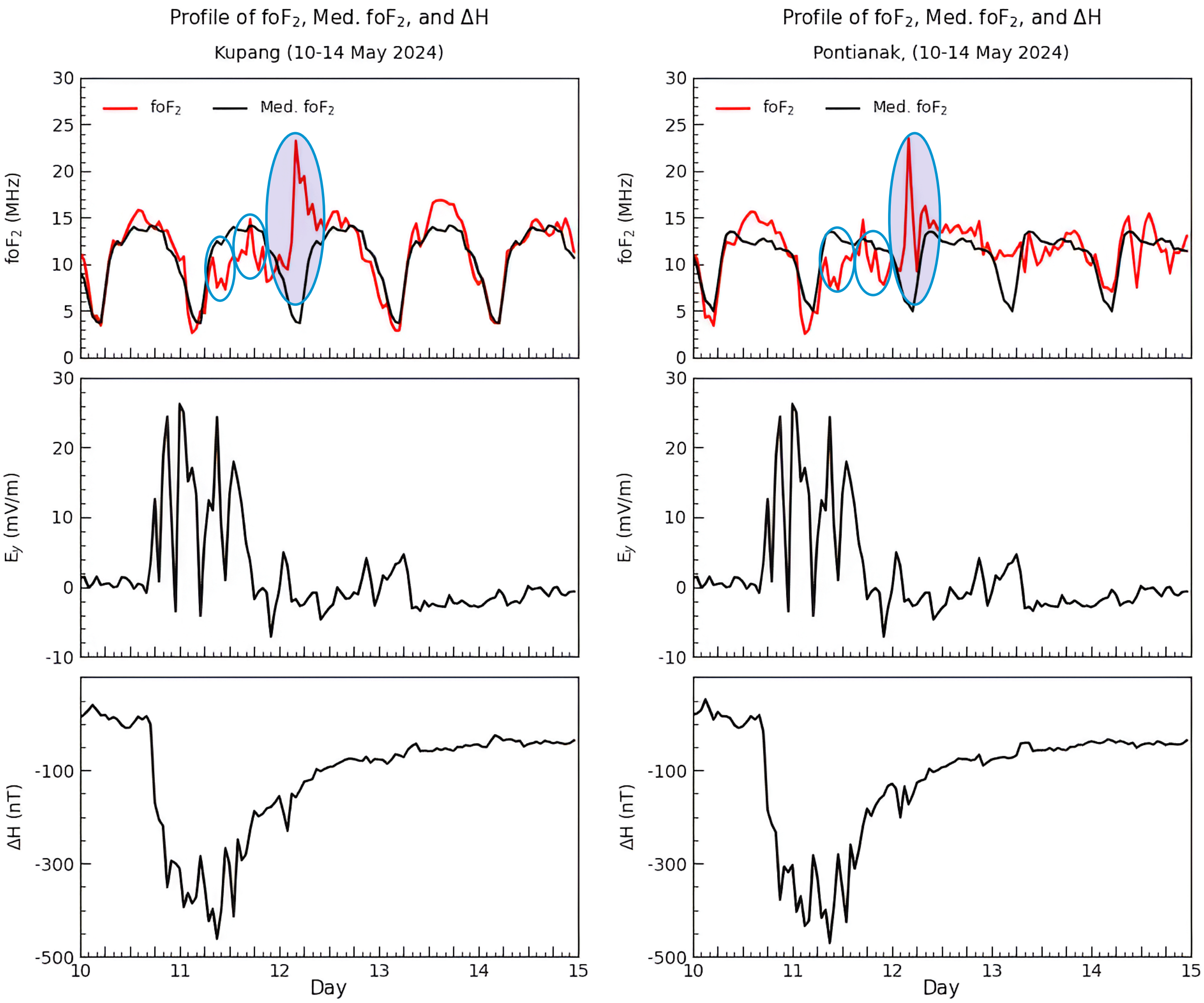

Figure 5. Graphical profile of *foF2*, Median *foF2*, *Ey* and *DH* from May 10-14. 2024 at Kupang (left) and Pontianak (right). The blue ellipse indicates the largest disturbances.

From **Figure 3**, it can be seen that geomagnetic disturbances in Indonesia caused by the geomagnetic storm on May 11, 2024, resulted in a minimum *ΔH* of -471 nT at KKI Kebun Raya BRIN Pontianak and a minimum *ΔH* of -462 nT at KSL Observatorium Nasional Timau BRIN Kupang. The minimum *ΔH* occurred at 08:00 UT on May 11, 2024 (or 16:00 WIB, Western Indonesian Time Zone, where WIB = UT + 7) for Pontianak and at 09:00 UT on May 11, 2024 (or 17:00 WIB, Center Indonesian Time Zone, where WITA = UT + 8) for Kupang. The geomagnetic *ΔH* amplitude at Pontianak and Kupang reached its minimum 7 hours after the peak of the geomagnetic storm on May 11, 2024 (*Dst* = -412 nT at 02:00 UT), possibly due to the delayed response of high-to-low latitude interaction processes (**Yumoto et al., 1996**). The *ΔH* amplitude at Pontianak was slightly greater than at Kupang, likely due to Pontianak's closer proximity to the magnetic equator, possibly experiencing a minor influence from the equatorial electrojet (EEJ). At the equator, the dynamo current causes an increase in Cowling conductivity generated by the magnetospheric convection electric field, leading to an increase in the eastward current during the daytime main phase of the geomagnetic storm. This highlights the role of the EEJ current at the equator, comparable to the Auroral Electrojet (*AE)* in polar regions. This finding aligns with the research of **Overbye (2013)**, **Ngwira and Pulkkinen (2018)**, **Tozzi et al. (2019)**, **Chakrabarty (2021)**, and **Nilam and Ram (2022)**.

From **Figure 4**, the amplitudes of *dD/dt, dH/dt, Ex* , and *Ey* for Pontianak (PTN) are 11.10 nT/min, 1.36 nT/min, 91.12 mV/km, and 9.45 mV/km, respectively. Meanwhile, for Kupang (KPG), the amplitudes of *dD/dt, dH/dt, Ex* , and *Ey* are 10.53 nT/min, 27.71 nT/min, 5.88 mV/km, and 29.04 mV/km, respectively. It can be seen that *Ex* and *Ey* at PTN are greater than at KPG. To further evaluate the potential for GIC in the Indonesian region, it is important to note the presence of a 500 kVA electricity distribution network across Java-Bali and Sumatra, spanning more than 100 km. The calculated in-

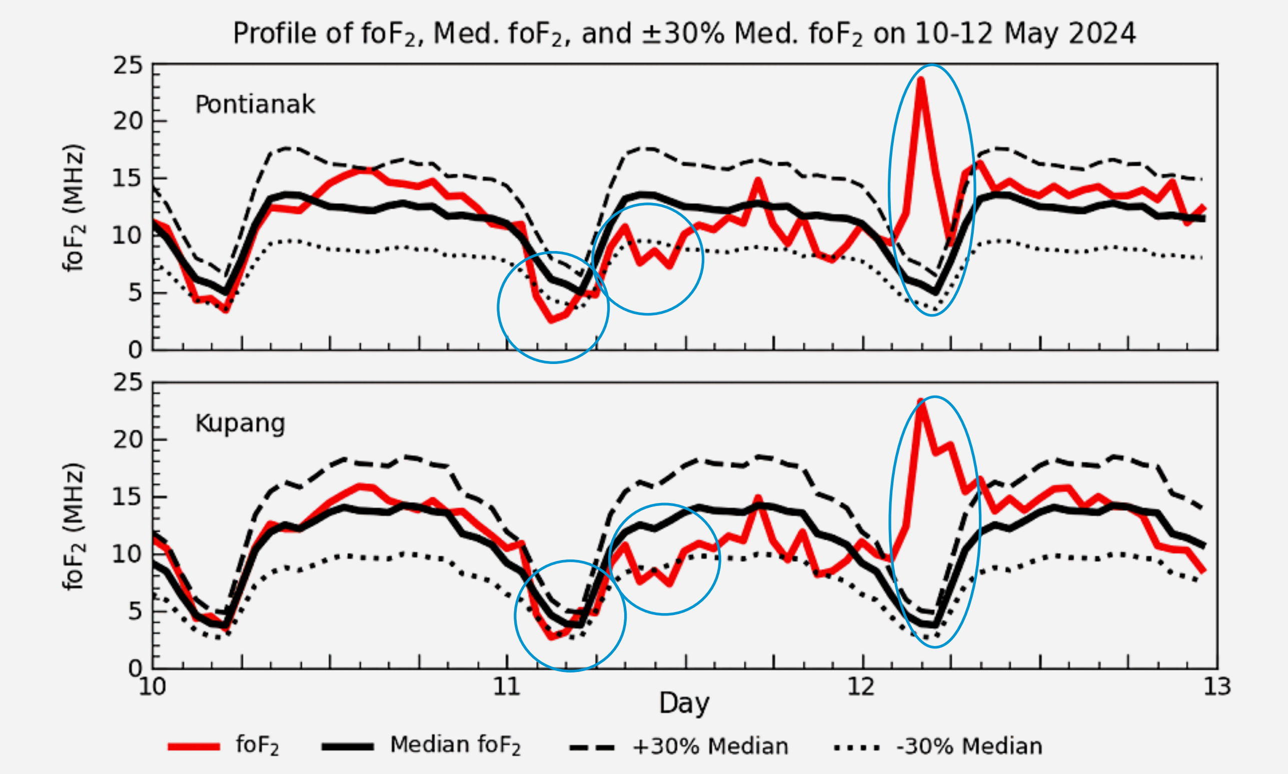

Figure 6. The profile of *foF2* data, the median, and ±30% of the median *foF2* value in Pontianak (top) and Kupang (bottom) from May 10 to 12, 2024. There are three regions where the value of ø < ±30% of the median *foF2* value, indicated by the blue circles/ellipses

duced electric fields for Pontianak (PTN) were on the order of 91.12 mV/km and 9.45 mV/km, respectively. Meanwhile, for Kupang (KPG), the amplitudes of *dD/dt, dH/dt, Ex*, and *Ey* were 10.53 nT/min, 27.71 nT/min, 5.88 mV/km, and 29.04 mV/km, respectively. However, no significant impacts were reported.

Resilience of Indonesia's Power Grid:

With an average distribution power of 1120 MVA (MW), the maximum current carried by the 500 kV transmission line is approximately 2240 A in alternating current (AC) (**Hidayat, 2021**). Therefore, the estimated overload current, as an anticipated overload, is 10% of 2240 A, which is about 224 A (AC). Meanwhile, GIC is quasi-DC. To date, the exact value of GIC in Indonesia remains unknown. However, referring to the research by **Zamawi et al. (2020)**, which simulated the maximum GIC capable of inducing half-cycle saturation in transformers, it was found that a GIC of 7 A was sufficient to trigger signs of half-cycle saturation. This finding explains why the GIC from the Mother's Day Storm did not cause disruptions or damage to Indonesia's power system.

From **Figure 6**, it is evident that both Pontianak and Kupang experienced a positive ionospheric storm during the main phase of the geomagnetic storm, followed by a negative storm during the recovery phase. On May 12, 2024, spread-F occurred at Pontianak (03:00 WIB or 07:00 UT) the increase in *fo*F2 value is about 23.52 MHz, and at Kupang (04:00 WITA or 08:00 UT) the increase in *fo*F2 value is about 23.22 MHz.

From **Figure 6**, a summary of the physical characteristics of the ionosphere in Pontianak and Kupang was obtained, and the results are presented in **Table 2**.

Based on **Table 2**, the ionospheric disturbances in Indonesia caused by the geomagnetic storm on May 11, 2024, lasted for 3 hours with a severity level of -30% > *f* > 30%, categorizing it as severe. The smallest *fo*F2 value is 2.51 MHz at 02:00 WIB on May 11, 2024 (18:00 UT on May 10, 2024) for Pontianak and 2.62 MHz at 03:00 WITA on May 11, 2024 (19:00 UT on May 10, 2024) for Kupang. Theoretically, it is known that MUF is three times *fo*F2 and OWF or FOT is 85% of MUF, so MUF values at PTN are about 3x2.15 MHz = 7.53 MHz and OWF or FOT is about 85% of MUF = 6.4 MHz. While the MUF value at KPG is about 3x2.62 MHz = 7.86 MHz and the OWF of FOT is about 85 of MUF = 6.68 MHz. These values are included in band 2 MHz – 30 MHz (ITU, 2019). However, no significant impacts on communication and navigation networks in Indonesia have been reported. Knowledge about the sources of signal interference and how to anticipate them is well understood by HF radio operators in Indonesia, and HF radio systems used in operational mode are modern communication as HF radio (**Wang et al., 2022**). As for satellite-based communication, operations have been effectively managed by satellite operators. This is likely

Table 1. Physical Characteristics of the Geospace Environment Before the Geomagnetic Storms on November 20, 2003 and May 11, 2024

No	Physical Characteristics	20-November-03	11-May-24
1	Flare class	M3.2	X2.2
2	Amount of Flare	1 flare on 18 November 2023 08:50 UT followed by halo CME	2 flares on 09 May 2024 Followed by halo CME
3	Linear Speed	1,660 km s^{-1}	08.45 UT - 1280 km s^{-1} and 18.52 UT – 1024 km s^{-1}
4	Kinetic Energy	3.3 × 10^{32} erg	-
5	Acceleration	-3.3 m s^{-2}	-20.6 m s^{-2}
6	Travel time	47.5 hours	32 hours
7	Dst minimum	-422 nT	-412 nT
8	Bz minimum	-50.9 nT	-35.3 nT
9	ΔT (B_{Zmin}-Dst_{min})	5 hours	2 hours
10	Value of *Nsw* when Dst reaching a minimum	18.8 N. cm^3	48.1 N. cm^3
11	ΔT (Nsw_{min}-Dst_{min})	9 hours	6 hours
12	Value of *Vsw* when Dst reaching a minimum	699 km s^{-1}	742 km s^{-1}
13	ΔT (Vsw_{max}-Dst_{min})	11 hours	2 hours
14	Value of *Psw* when Dst reaching a minimum	18.37 nPa	55.89 nPa
15	ΔT (Psw_{max}-Dst_{min})	11 hours	6 hours
16	$ΔT_{Dst}$ onset to minimum	14 hours	11 hours

ΔT (Bz_{min}-Dst_{min}) is the time lag between minimum *Bz* and minimum *Dst, ΔT* (Nsw_{max}-Dst_{min}) is the time lag between maximum Nsw and minimum *Dst*, *ΔT* (Vsw_{max}-Dst_{min}) is time lag between maximum *Vsw* and minimum *Dst, ΔT* (Psw_{max}-Dst_{min}) is time lag between maximum *Psw, Bz* and minimum *Dst*

Table 2. Summary of ionospheric irregularity characteristics over Pontianak and Kupang from May 10-12, 2024

No	Physical Characteristics	Values	
		Pontianak	Kupang
a	The amount of -30% Median < $foF2_{data}$	3 times	2 times
b	The value of $foF2_{data}$ has long been in position a.	3 hours, 3 hours and 1 hour	3 hours and 1 hour
c	The time of occurrence of $foF2_{data}$ is at position a.	02:00-04:00 LT; 09:00-11:00 LT and 22:00 LT	09:00-11:00 LT and 19:00 LT
d	The date of occurrence of $foF2_{data}$ is at position a.	On May 11, 2024	On May 11, 2024
e	The amount of $foF2_{data}$ > 30% Median	2 times	1 time
f	The value of $foF2_{data}$ has long been in position e.	3 hours and 1 hour	7 hours
g	The time of occurrence of $foF2_{data}$ is at position e.	03:00-05:00 LT and 07:00 LT	02:00-08:00 LT
h	The date of occurrence of $foF2_{data}$ is at position e.	On May 12, 2024	On May 12, 2024

why the impact of the Mother's Day Storm did not significantly affect the Indonesian region.

5. Conclusions

From the discussion above, it can be concluded that the conditions and behaviours of solar wind parameters, along with *Bs (Bz* which is southward direction), play a critical role in determining the intensity of geomagnetic storms. Their combination is essential for the occurrence (or absence) of geomagnetic storms and also influences their intensity. Based on the case studies of two geomagnetic storm events, we conclude that the duration and intensity of Bs are key factors that facilitate the entry of solar wind parameters into the Earth's magnetosphere.

The geomagnetic storm on May 11, 2024, caused geomagnetic disturbances with *ΔH* = -471 nT in Pontianak (severe storm) and *ΔH* = -462 nT in Kupang (severe storm) while the geoelectric disturbances of E_x = 91.12 mV/km and E_y = 9.45 mV/km (in Pontianak) and E_x = 5.88 mV/km and E_y = 29.04 mV/km (in Kupang) were observed. In the ionosphere, the geomagnetic storm caused negative ionospheric storms during the main phase and positive storms during the recovery phase, as observed in the *fo*F2 data from Pontianak and Kupang. These ionospheric storms resulted in severe *fo*F2 disturbances (ϕ) with values ranging from -30% to 30%, lasting for 180 minutes.

Acknowledgement

The authors thank the Head of the Research Center for Space, the PhD Degree by Research program promotor, co-promotor, for supporting the study. The authors also thank the Coordinator of KKI Kebun Raya Pontianak - BRIN for providing *fo*F2 and geomagnetic field data, the Coordinator of KST Obnas Timau - BRIN and KSL Stasiun Observasi Agam for geomagnetic field data. We acknowledge the CDAWeb https://omniweb.gsfc.nasa.gov/form/dx1.html for providing solar wind and *Bz* data, WDC for geomagnetics Kyoto https://wdc.kugi.kyoto-u.ac.jp/wdc/Sec3.html for providing the *Dst* index data, the UMD space Physics group https://space.umd.edu/pm/figs/figs.html and NASA https://cdaw.gsfc.nasa.gov/CME_list/ for providing CME event data, the GFZ Postdam https://datapub.gfz-postdam.de/donwload/10.5880.Kp.0001/Quiet_Disturbed_Days/QD_days2024.txt for providing International Quiet Days data, the Geological Agency of Indonesian Ministry of Energy and Mineral Resources https://geoportal.esdm.go.id/geologi/ for Indonesia's Geological data and all researchers in Space Weather Information and Forecast Services (SWIFtS), Research Center for Space, ORPA-BRIN for their contributions, both direct and indirect.

6. References

Abadi, P., Otsuka, Y., Liu, H., Hozumi, K., Martinigrum, D. R., Jamjareegulgarn, P., and Otadoy, R. (2021). Roles of thermospheric neutral wind and equatorial electrojet in pre-reversal enhancement, deduced from observations in Southeast Asia. Earth and Planetary Physics, 5(5), 387-396. https://doi.org/10.26464/epp2021049

Abda, Z. M. K., Ab Aziz, N. F., Ab Kadir, M. Z. A., and Rhazali, Z. A. (2020). A review of geomagnetically induced current effects on electrical power system: Principles and theory. IEEE Access, 8, 200237-200258. DOI: 10.1109/ACCESS.2020.3034347

Akala, A. O., Oyeyemi, E. O., Amaechi, P. O., Radicella, S. M., Nava, B., and Amory-Mazaudier, C. (2020). Longitudinal responses of the equatorial/low-latitude ionosphere over the oceanic regions to geomagnetic storms of May and September 2017. Journal of Geophysical Research: Space Physics, 125(8), e2020JA027963. https://doi.org/10.1029/2020JA027963

Balan, N., Liu, L., and Le, H. (2018). A brief review of equatorial ionization anomaly and ionospheric irregularities. Earth and Planetary Physics, 2(4), 257-275.

Carr J. J. (2011). Practical Antenna Handbook 5/e, ISBN 978-0-07-163958-3

Chakrabarty D. (2021). Penetration Electric Fields: Meaning, Nature, Importance and Complexities, Session 3: Space Weather Impacts on Magnetosphere -Thermosphere -Ionosphere System ISWI Workshop on Space Weather: Science and Applications jointly organized by the UNOOSA and VSSC, ISRO 2 –3 November 2021

Cliver, E. W., Schrijver, C. J., Shibata, K., and Usoskin, I. G. (2022). Extreme solar events. Living Reviews in Solar Physics, 19(1), 2. https://doi.org/10.1007/s41116-022-00033-8

Foster, J. C., Erickson, P. J., Nishimura, Y., Zhang, S. R., Bush, D. C., Coster, A. J., and Franco-Diaz, E. (2024). Imaging the May 2024 extreme aurora with ionospheric total electron content. Geophysical Research Letters, 51(20), e2024GL111981. https://doi.org/10.1029/2024GL111981

Goodman, J. M. (1992). HF Communications Science and Technology, Van Nostrand Reinhold, New York.

Gopalswamy, N., Barbieri, L., Cliver, E. W., Lu, G., Plunkett, S. P., and Skoug, R. M. (2005). Introduction to violent Sun-Earth connection events of October–November 2003. Journal of Geophysical Research: Space Physics, 110(A9). https://doi.org/10.1029/2005JA011268

Grandin, M., Bruus, E., Ledvina, V. E., Partamies, N., Barthelemy, M., Martinis, C., ... and Bergstrand, C. (2024). The geomagnetic superstorm of 10 May 2024: Citizen science observations. EGU sphere, 2024, 1-32. https://doi.org/10.5194/egusphere-2024-217

Hajra, R., Tsurutani, B. T., Lakhina, G. S., Lu, Q., and Du, A. (2024). Interplanetary causes and impacts of the 2024 may superstorm on the geosphere: An overview. The Astrophysical Journal, 974(2), 264. DOI: 10.3847/1538-4357/ad7462

Hapgood, M. A. (2011). Towards a scientific understanding of the risk from extreme space weather. Advances in Space Research, 47(12), 2059-2072. https://doi.org/10.1016/j.asr.2010.02.007

Hidayat A. (2021). Tingkatkan Keandalan Listrik Pulau Jawa, PLN Operasikan SUTET 500 kV PLTU Tanjung Jati B – Pemalang (Batang) dan GITET 500 kV Pemalang (Batang), Press Release No. 225.PR/STH.00.01/I/2021, https://web.pln.co.id/cms/media/siaran-pers/2021/06/tingkatkan-keandalan-listrik-pulau-jawa-pln-operasikan-sutet-500-kv-pltu-tanjung-jati-b-pemalang-batang-dan-gitet-500-kv-pemalang-batang/, read on 12 February 2015.

Horvarth I., and Lovell B. C. (2015). Positive and negative ionospheric storms occurringduring the 15 May 2005 geomagnetic superstorm, JGR: Space Physics, https://doi.org/10.1002/2015JA021206

Ishii, M., Berdermann, J., Forte, B., Hapgood, M., Bisi, M. M., and Romano, V. (2024). Space weather impact on radio communication and navigation. Advances in Space Research. https://doi.org/10.1016/j.asr.2024.01.043

ITU. (2007). ITU-R P.373-8. (2007). Definitions of maximum and minimum transmission frequencies. https://www.itu.int/rec/R-REC-P.373-9- 201309-I/en

ITU. (2015). Recommendation ITU-R V.431-8 Nomenclature of the frequency and wavelength bands used in telecommunications, Recommendation. https://www.itu.int/rec/R-REC-V.431-8-201508-I/en

ITU. (2019). Recommendation ITU-R P.533-14 Method for the prediction of the performance of HF circuits, Recommendation. https://www.itu. int/rec/R-REC-P.533-14-201908-I/en

Jaswal, P., Sinha, S., and Nandy, D. (2024). Deconstructing solar super active region 13664 in the context of Historic Geomagnetic storm of 2024 May 10-11. *arXiv2409.14752v1* [astro-ph.SR] 23 Sep 2024 https://doi.org/10.3847/1538-4357/ad960b

Jatmiko H. B., trihasto A., Pravitasari D. (2024). Evaluasi Ketidakseimbangan Beban Terhadap Arus Netral Pada Transformator Di Gardu Induk 150 Kv Secang, RELE : Jurnal Teknik Elektro, Vol. 7 No. 1. ISSN 2622-7002.

Karan, D. K., Martinis, C. R., Daniell, R. E., Eastes, R. W., Wang, W., McClintock, W. E., ... and England, S. (2024). GOLD observations of the merging of the Southern Crest of the equatorial ionization anomaly and aurora during the 10 and 11 May 2024 Mother's Day super geomagnetic storm. Geophysical Research Letters, 51(15), e2024GL110632. https://doi.org/10.1029/2024GL110632

Kwak, Y. S., Kim, J. H., Kim, S., Miyashita, Y., Yang, T., Park, S. H., ... and Talha, M. (2024). Observational Overview of the May 2024 G5-Level Geomagnetic Storm: From Solar Eruptions to Terrestrial Consequences. Journal of Astronomy and Space Sciences, 41(3), 171-194. https://10.5140/JASS.2024.41.3.171

Kontogiannis, I. (2024). The extremely strong non-neutralized electric currents of the unique solar active region NOAA13664. Astronomy and Astrophysics, 690, L10. https://10.1051/0004-6361/202451627

Liu C, Liu L, and Yang Y. (2009). Monitoring and modeling geomagnetically induced currents in power grids of China. Paper presented at 2009 Asia-Pacific Power and Energy Engineering Conference, Wuhan, China, 27–31 March 2009. https://doi.org/10.1109/APPEEC.2009.4918502

Liu, Y. D., Hu, H., Zhao, X., Chen, C., and Wang, R. (2024). A Pileup of Coronal Mass Ejections Produced the Largest Geomagnetic Storm in Two Decades. The Astrophysical Journal Letters, 974(1), L8. DOI: 10.3847/2041-8213/ad7ba4

Love J. J. (2020). Some experiments in extreme-value statistical modeling of magnetic superstorm intensities. Space Weather 18:e02255. https://doi.org/10.1029/2019SW002255

Marshall RA, Gorniak H, Walt TVD, Waters CL, Sciffer MD, Miller M, Dalzell M, Daly T, Pouferis G, Hesse G, and Wilkinson P. (2013). Observations of geomagnetically induced currents in the Australian power network. Space Weather 11(1):6–16. https://doi.org/10.1029/2012SW000849

Matamba, T.M., Habarulema, J.B., and McKinnell, L.A. (2015). Statistical analysis of the ionospheric response during geomagnetic storm conditions over South Africa using ionosonde and GPS data. Space Weather 13, 536–547

Matzka, J., Stolle, C., Yamazaki, Y., Bronkalla, O., and Morschhauser, A. (2021). The geomagnetic Kp index and derived indices of geomagnetic activity. Space weather, 19(5), e2020SW002641. https://doi.org/10.1029/2020SW002641

Ngwira C. M., Pulkkinen A., Wilder F. D., and Crowley G. (2013). Extended study of extreme geoelectric field event scenarios for geomagnetically induced current applications, SPACE WEATHER, VOL. 11, 121–131, https://doi:10.1002/swe.20021

Ngwira C. M., and Pulkkinen A. A. (2018). An overview of science challenges pertaining to our understanding of extreme geomagnetically induced currents, in Extreme Events in Geospace. Amsterdam, The Netherlands: Elsevier, 2018, pp. 187_208 https://doi.org/10.1016/B978-0-12-812700-1.00008-X

Nilam B., and S. T. Ram. (2022). Large Geomagnetically Induced Currents at Equator Caused by an Interplanetary Magnetic Cloud, Space Weather. https://doi.org/10.1029/2022SW003111

Overbye T.. (2013). Power grid geomagnetic disturbance (GMD) modeling with transformer neutral blocking and live grid testing results. in Proc. CPE- Conf./MIPSY Con-Paper. 2013. pp. 1_8. https://doi.org/10.1109/EPEC.2013.6802963

Parker, W. E., and Linares, R. (2024). Satellite Drag Analysis During the May 2024 Gannon Geomagnetic Storm. Journal of Spacecraft and Rockets, 61(5), 1412-1416. https://doi.org/10.2514/1.A36164

Pulkkinen, A., Bernabeu, E., Thomson, A., Viljanen, A., Pirjola, R., Boteler, D., and MacAlester, M. (2017). Geomagnetically induced currents: Science, engineering, and applications readiness. Space weather, 15(7), 828-856. DOI: 10.1002/2016SW001501

Riley, P., Baker, D., Liu, Y. D., Verronen, P., Singer, H., and Güdel, M. (2018). Extreme space weather events: From cradle to grave. Space Science Reviews, 214, 1-24. https://doi.org/10.1007/s11214-017-0456-3

Spogli, L., Alberti, T., Bagiacchi, P., Cesaroni, C., Coco, I., Di Mauro, D., and Tozzi, R. (2024). The effects of the May 2024 Mother's Day superstorm over the Mediterranean sector: from data to public communication. Authorea Preprints. https://doi.org/10.4401/ag-9117

Themens, D. R., Elvidge, S., McCaffrey, A., Jayachandran, P., Coster, A., Varney, R. H., and Reid, B. (2024). The high latitude ionospheric response to the major May 2024 geomagnetic storm: A synoptic view. Geophysical Research Letters, 51(19), e2024GL111677. https://doi.org/10.1029/2024GL111677

Torta JM, Serrano L, Regue JR, Sanchez AM, and Roldan E. (2012). Geomagnetically induced currents in a power grid of northern Spain. Space Weather 10(6):S06002. https://doi.org/10.1029/2012SW000793

Tozzi R., Coco I., Michelis P. D., and Giannattasio F. (2019). Latitudinal Dependence Of Geomagnetically Induced Currents During Geomagnetic Storms. Annals Of Geophysics. 62. 4. GM448. 2019; https://doi.org/10.4401/ag-7788

Trivedi NB, Vitorello I, Kabata W, Dutra SLG, Padilha AL, Bologna MS, de Padua MB, Soares AP, Luz GS, FdeA P, Pirjola R, and Viljanen A. (2007). Geomagnetically induced currents in an electric power transmission system at low latitudes in Brazil: a case study. Space Weather 5(4):S04004. https://doi.org/10.1029/2006SW000282

Tsubouchi, K., and Omura, Y. (2007). Long-term occurrence probabilities of intense geomagnetic storm events. Space Weather, 5(12), S12003. https://doi.org/10.1029/2007SW000329

Viljanen A. (1998). Relation of Geomagnetically Induced Currents and Local Geomagnetic Variations, IEEE Transaction on Power Delivery, Vol. 13 No. 4, https://doi.org/10.1109/61.714497

Wang J., Shi Y., Yang C., and Feng F. (2022). A review and prospects of operational frequency selecting techniques for HF radio communication, Advances in space research, 69, 2989-2999. https://doi.org/10.1016/j.asr.2022.01.026

Watari S, Kunitake M, Kitamura K, Hori T, Kikuchi T, Shiokawa K, Nishitani N, Kataoka R, Kamide Y, Aso T, Watanabe Y, and Tsuneta Y. (2009). Measurements of geomagnetically induced current in a power grid in Hokkaido. Japan Space Weather 7(3):S03002. https://doi.org/10.1029/2008SW000417

Watari, S., Nakamura, S., and Ebihara, Y. (2021). Measurement of geomagnetically induced current (GIC) around Tokyo, Japan (Vol. 73, pp. 1-19). https://doi.org/10.1186/s40623-021-01422-3

Yumoto K., and the 210° MM Magnetic Observation Group. (1996). The STEP 210° Magnetic Meridian Network Project, J. Geomag. Geoelectr, 48, 1297-1309. https://doi.org/10.5636/jgg.47.1197

Zawawi A. A., Ab Aziz, N. F., Ab Kadir M. Z. A., Hashim H., and Muhammed Z. (2020). Evolution of geomagnetic induced current on 275 kV power transformer for a reliable and sustainable power system operation in Malaysia, Sustainability, MDPI, Sustainability 2020, 12, 9225. https://doi.org/10.3390/su12219225

SAŽETAK

Procjena učinaka jake geomagnetske oluje od 10. do 11. svibnja 2024. na geomagnetsko polje i ionosferu nad indonezijskim područjem

Jaka geomagnetska oluja 11. svibnja 2024. najveći je svemirski vremenski fenomen u 25. Sunčevu ciklusu. U ovome radu prikazan je utjecaj te jake geomagnetske oluje (*Dst* = −412 nT) na geomagnetsko polje i ionosferu iznad Indonezije. Dodatno, ispituju se geoelektrični poremećaji nastali tijekom oluje i poremećaji HF radiokomunikacije u Indoneziji. Studija upotrebljava podatke o geomagnetskome polju (HDZ) i podatke o ionosferi (*fo*F2) iz Pontianaka i Kupanga, izračunane u prosjeku po minuti i po satu. Rezultati pokazuju da je geomagnetska oluja 11. svibnja 2024. uzrokovala geomagnetske poremećaje s ΔH = −471 nT u Pontianaku i ΔH = −462 nT u Kupangu. Ti su poremećaji doveli do znatnih geoelektričnih potresa oko regije s mogućim induciranim strujama. U ionosferi je geomagnetska oluja uzrokovala negativne ionosferske oluje tijekom glavne faze i pozitivne oluje tijekom faze oporavka, kao što je primijećeno u *fo*F2 podatcima s obiju postaja. Ove ionosferske oluje rezultirale su poremećajima *fo*F2 (ø) s vrijednostima u rasponu od −30 % do 30 % u trajanju od 180 minuta.

Ključne riječi:
geomagnetska oluja, međuplanetarno magnetsko polje, svemirsko vrijeme, geomagnetska inducirana struja, ionosfera

Author's contribution

Anwar Santoso (Doctoral Student of Physics, first author, magnetosphere and ionosphere) provided analyses and interpretations on the geomagnetic storm and its effect on geomagnetic field and ionosphere. **Sismanto** (Promotor, co-author, Earth electric field-Physics) provided lithospheric potential on geomagnetic induced current analysis. **Rhorom Priyatikanto** (Co-Promotor-1, Doctor of Astronomy and Astrophysics, Co-author, Astronomy and Astrophysics) provided solar activity analyses. **Eddy Hartantyo** (Co-Promotor-2, Doctor of Physics, Co-author, Physics) provided geological analyses. **Emanuel Sungging Mumpuni** (Doctor of Astronomy and Astrophysics, Co-author, Astronomy and Astrophysics) provided solar activity interpretations. **La Ode Muhammad Musafar Kilowasid** (Doctoral Student of Physics, co-author, magnetosphere and ionosphere) provided ionosphere and geomagnetic field data and interpretation at KKI Kebun Raya BRIN Pontianak. **Abdul Rahman** (Doctor of Astronomy and Astrophysics, Co-author, Astronomy and Astrophysics) provided ionosphere and geomagnetic field data interpretation at KSL Observasi Nasional Timau BRIN Kupang. **Fitri Nuraeni** (Master of Physics, Co-author, magnetosphere and ionosphere) provided analyses and interpretations of the geomagnetic data. **Siska Filawati** (Master of Physics, Co-author, magnetosphere and ionosphere) contributed in geomagnetic data processing and figure generation. **Erlansyah** (Master of Physics, Co-author, magnetosphere and ionosphere) contributed on ionospheric data interpretation. **Dadang Nurmali** (Bachelor of Physics, Co-author, magnetosphere and ionosphere) contributed on ionosphere data processing.
All authors have read and agreed to the published version of the manuscript.